Journal of Propulsion and Energy Vol. 3, No. 1. October 2022; 3(1): 51-60
https://doi.org/10.6108/JPNE.2022.3.1.051
pISSN 2734-1887 eISSN 2765-0049

JPNE

Comparison of the Semi-empirical Heat Transfer Coefficient for a Liquid Rocket Nozzle with Regenerative Cooling Jacket

Jongmin Shin [a] · **Tae-Seong Roh** [a] · **Hyoung Jin Lee** [a,*]

[a] Department of Aerospace Engineering, Inha University, Incheon 21999 Korea

Corresponding author [*]
Hyoung Jin Lee
hyoungjin.lee@inha.ac.kr

Received : 16 December 2021
Revised : 15 February 2022
Accepted : 21 February 2022

The heat transfer phenomenon of a liquid rocket engine has been studied using various equations for heat transfer coefficients. The heat transfer coefficient can be calculated using Prandtl-Taylor analogy and Bartz's empirical equation, and its variations. Through 1D analysis of a liquid rocket engine with a regenerative cooling jacket, the effects of heat transfer coefficients with various semi-empirical equations were analyzed. The difference in heat transfer coefficient affects the heat transfer such as heat flux, gas-side wall temperature, pressure of coolant, and temperature of the coolant. The analysis results were compared to the result by CFD simulation to evaluate the characteristics of semi-empirical equations. The results showed that the heat transfer of a nozzle with regenerative cooling jacket could be simulated well through 1D cooling channel analysis. In addition, the modified Bartz equation showed the best result among various empirical equations.

Key Words: Heat Transfer Coefficient, Bartz Equation, Supersonic Nozzle, Regenerative Cooling

1. Introduction

In most rocket systems, the heat generated by combustion is needed to improve thrust performance. Some rockets use heat-resistant materials or radiant cooling without any cooling system when burning time is short enough. However, in a liquid rocket with long and continuous burning time, a cooling system to protect the chamber and nozzle from heat is essential. There are various cooling methods applied to the liquid rocket system, but two main methods are widely used representatively: film cooling and regenerative cooling. Film cooling uses a coolant to protect the inner wall of the combustion chamber and nozzle from the high-temperature combustion gas. Both gas and liquid fluids can be used for cooling, non-combustible helium as a gas coolant, and liquid fuel and liquid oxidizer as liquid coolant [1]. Exhaust and regenerative cooling are methods that lower the temperature of the hot inner wall by passing a coolant through a cooling

channel between the inner and outer walls of the combustion chamber and nozzle. The coolant is discharged to the outside without being reused in an exhaust cooling method. However, in the case of regenerative cooling method, a heated coolant is used to operate the turbine or is injected through the injector and used as a propellant. It is necessary to ensure adequate cooling performance while satisfying the requirements of each engine part. For this purpose, it is necessary to accurately predict the properties of the coolant that have passed through the cooling channel.

For an accurate design of the cooling channel, Pizzarelli et al. compared the heat transfer coefficient based on the curvature of the cooling channel, pressure drop, and temperature increase of the coolant through computational simulations [2]. Ulas et al. observed that the gas-side wall temperature, coolant temperature, and pressure drop differ depending on height-to-width aspect ratio of the cooling channel and the number of cooling channels [3]. The results showed that as the aspect ratio increased, the gas-side wall temperature significantly decreased, and the pressure drop through the cooling channel increased. Cavillon et al. confirmed that the elliptical cross-sectional configuration of the cooling channel had a higher heat transfer coefficient than the rectangular channel through computational simulations [4]. Betti conducted a heat transfer analysis of the nozzles and cooling channels of the LOX/CH_4 theoretical engine with an expander cycle using CFD simulations with the Bartz equation [5-6]. The differences in the heat transfer coefficient, heat flux, gas-side wall temperature, coolant temperature, and pressure were reported.

The convective heat transfer coefficient in the cooling channel analysis was used to predict heat transfer between the combustion gas and the inner wall, as well as between the inner wall and coolant. The Reynolds analogy, the Prandtl-Taylor analogy, the Bartz's semi-empirical equations, and the Dittus-Boelter equation can be used to predict convective heat transfer. And it is well-known that each equation has different results under the same conditions. However, among the semi-empirical equations, the evaluation on the regenerative cooling characteristics for a liquid rocket system was not performed, and even comparison with the CFD results has not been reported. In this study, the effect of various semi-empirical heat transfer coefficients on regenerative cooling characteristics was analyzed. To this end, 1D heat transfer analysis of a regenerative cooling system using liquid methane fuel was performed by applying various semi-empirical equations, and compared with previously performed CFD results.

2. Semi-empirical Heat Transfer Coefficient

Heat transfer analysis of the cooling channel is required to predict the wall temperature and coolant properties of the regenerative cooling channel. A proper heat transfer coefficient should be used to conduct heat transfer analysis. As mentioned in the introduction, semi-empirical equations and corrected equations have been reported and used. In this section, the semi-empirical equations are briefly explained, and the methods used to evaluate the characteristics of the equations are summarized and presented.

The Reynolds analogy is based on a similar relationship between momentum and heat transfer in the boundary layer. As shown in (Eq. 1) and (Eq. 2), the heat transfer coefficient was expressed as a surface friction coefficient function.

$$h = \frac{C_f}{2}\rho u C_p \tag{1}$$

$$\frac{C_f}{2} = \frac{0.023}{Re_D^{0.2}} \tag{2}$$

However, the Eq. 1 does not hold when the Pr is not unity, which corresponds to an actual nozzle flow, such as rockets. However, the Prandtl-Taylor analogy expresses the heat transfer coefficient as follows (Eq. 3) by applying the heat conduction equation in the sublayer of the boundary layer and Reynolds analogy in turbulent flow.

$$h = \rho u C_p \frac{C_f/2}{1+5\sqrt{C_f/2}\,(Pr-1)} \quad (3)$$

In 1957, Bartz presented a semi-empirical equation (Eq. 5) using the Nusselt number (Eq. 4) for heat transfer analysis inside a supersonic nozzle [7].

$$Nu = C(Re)^m(Pr)^n \quad (4)$$

$$h_g = \left[\frac{0.026}{D_*^{0.2}}\left(\frac{\mu_c^{0.2}C_p}{Pr^{0.6}}\right)\left(\frac{P_c}{C^*}\right)^{0.8}\right]\left(\frac{A_*}{A}\right)^{0.9}\sigma \quad (5)$$

In Eq. 4, $C = 0.026$, $m = 0.8$ and $n = 0.4$ were applied for Eq. 5, and σ represents the correction factor for the change in the property values inside the boundary layer of the nozzle. After a correction factor, $(D_*/r_c)^{0.1}$ for the curvature configuration of the nozzle was added to Eq. 5, and Eq. 6 has been presented [7, 8].

The correction factor σ (Eq. 7), $\omega = 0.6$ was suggested by Huzel et al. [9], and Eq. 8 can be derived using Eq. 6-7 without ω. ρ_{ref} and μ_{ref} ref are the values at the intermediate position between the wall and center of the nozzle, however in this study, the values at the central axis were assumed and applied for 1D analysis.

$$h_g = \left[\frac{0.026}{D_*^{0.2}}\left(\frac{\mu_c^{0.2}C_p}{Pr^{0.6}}\right)\left(\frac{P_c}{C^*}\right)^{0.8}\left(\frac{D_*}{r_c}\right)^{0.1}\right]\left(\frac{A_*}{A}\right)^{0.9}\sigma \quad (6)$$

$$\begin{aligned}\sigma &= \left[\left(\frac{\rho_{ref}}{\rho}\right)^{0.8}\left(\frac{\mu_{ref}}{\mu_c}\right)^{0.2}\right] \\ &= \left[\frac{1}{2}\frac{T_{wg}}{T_0}\left(1+\frac{\gamma-1}{2}M^2\right)+\frac{1}{2}\right]^{-\left(0.8-\left(\frac{\omega}{5}\right)\right)} \\ &\quad \times\left[1+\frac{\gamma-1}{2}M^2\right]^{-(\omega/5)}\end{aligned} \quad (7)$$

$$h_g = 0.026\mu_{ref}^{0.2}C_p^{0.4}\left(\frac{k}{\mu_{ref}}\right)^{0.6}\left(\frac{\dot{m}^{0.8}}{A^{0.9}}\right)\left(\frac{\pi D_*}{4r_c}\right)^{0.1} \quad (8)$$

In 1966, Pavli et al. applied $C = 0.023$, $m = 0.8$, and $n = 0.4$ in Eq. 4, and a temperature correction factor (K_T) was added [10]. In the derivation process of Eq. 9, K_T (Eq. 10) is included in Re of Eq. 4; therefore, the exponent of K_T was set to $e = 0.8$. T_0 denotes the temperature at the nozzle axis.

$$h_g = 0.023Re^{-0.2}Pr^{-0.6}C_p\left(\frac{\dot{m}}{A}\right)K_T \quad (9)$$

$$K_T = \left(\frac{T_{aw}}{T_{ref}}\right)^e, T_{ref} = \frac{T_0+T_{wg}}{2} \quad (10)$$

$$h_g = 0.026\mu_{ref}^{0.2}C_p^{0.4}\left(\frac{k}{\mu_{ref}}\right)^{0.6}\left(\frac{\dot{m}^{0.8}}{A^{0.9}}\right)\left(\frac{\pi D_*}{4r_c}\right)^{0.1}K_T \quad (11)$$

$$K_T = \left(\frac{T_{aw}}{T_{ref}}\right)^a, T_{ref} = \frac{T_0+T_{wg}}{2} \quad (12)$$

The semi-empirical equation for the heat transfer coefficient presented by Astrium et al. is the addition of a temperature correction factor (K_T) and a configuration correction factor (K_X) to the Bartz equation of Eq. 8 [11]. In this study, because the equation with the configuration correction factor is known to be uncertain, Eq. 11 with only the temperature correction factor (K_T) was used [11-13]. The exponent (a) of the temperature correction factor (Eq. 12) was not presented as a specific value [11], however from the analysis result of this study, when $a = 0.2$ was used, the gas-side wall temperature result of the cooling channel analysis was similar to the analysis result of Betti [5].

3. Result and Discussion

For a regenerative cooling nozzle of a liquid rocket, 1D analysis was performed on the nozzle and cooling channel designed by Schuff et al. [6] using a semi-empirical equation for the heat transfer coefficient. The results were validated by comparison to the results obtained using a commercial analysis program named Rocket Propulsion Analysis (RPA) and Betti [5]'s CFD results.

3.1 Analysis target

The nozzle and cooling channel used for validating the heat transfer analysis procedure of the regenerative cooling nozzle was a 25000 lbf liquid methane engine designed by Schuff et al. [6], and liquid methane, a

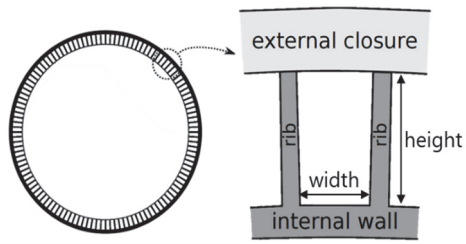

Fig. 1. Cross-sectional configuration of cooling channel sectionominations.

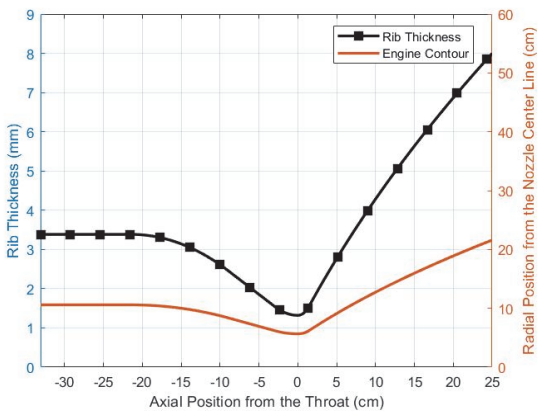

Fig. 2. Engine dimension and rib thickness of cooling channel.

cryogenic fuel, was used as the coolant. The cross-sectional configuration and every component of the cooling channel jacket are shown in Fig. 1, and the specifications of the nozzle and cooling channel are presented in Tables 1 and 2.

The expansion ratio of the engine nozzle was 180, however the cooling channel existed only from the combustion chamber to the position with an area ratio of 15. In addition, the horizontal and vertical lengths of the cooling channel are constant; therefore, the rib thickness of the channel changes according to position, as shown in Fig. 2. RPA, a CEA-based commercial program, was used to obtain the properties of hot gas required for the cooling channel analysis, and the simulation results obtained using 1D cooling channel analysis from RPA were also used for comparison and validation. To validate the present 1D analysis and compare the characteristics of the heat transfer coefficient, a semi-empirical formula (Eq. 3, 5, 6, 8, 9, and 11) introduced in Section 2 were used. The results are shown in Figs. 5-8. The heat flux, gas-side wall temperature, coolant temperature, coolant pressure, and heat transfer coefficient by the axial position of the nozzle are presented.

Table 1. Specifications and conditions of 25000 lbf liquid methane engine with regenerative cooling nozzle.

Chamber Pressure (bar)	58.6
Adiabatic Flame Temperature (K)	3603.2
Mixture Ratio (O/F)	3.5
Throat Radius (cm)	5.66
Expansion Ratio	180
Contraction Ratio	3.5
Divergent Section Length (cm)	223
Convergent Section Length (cm)	33.1
Characteristic Length (cm)	88.9

Table 2. Specifications and conditions of 25000 lbf liquid methane engine's cooling channel.

Inlet Coolant Pressure (bar)	127
Inlet Coolant Temperature (K)	120
Channel Width (mm)	1.08
Channel Height (mm)	8.63
Internal Wall Thickness (mm)	0.7
Channel Aspect Ratio	8
Number of Channels	150
Inlet Section Abscissa (cm)	25.1
Inlet Section Area Ratio	15

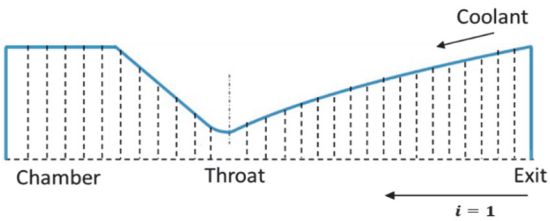

Fig. 3. Direction of coolant flow and simulation.

3.2 Analysis procedure

The regenerative cooling nozzle used in this study is a conventional convergent/divergent nozzle applied to rockets and has the configuration shown in Fig. 3, and the coolant moves from the nozzle exit to the combustion chamber. In the analysis of the cooling channel of the regenerative cooling nozzle, the heat transfer coefficient from the hot gas to the inner wall of the nozzle is one of the main factors that determines the heat flux. Therefore, the analysis procedure for the cooling channel was used to evaluate the semi-empirical equation used to derive the heat transfer coefficient.

The analysis procedure used in this study is shown in Fig. 4 The inputs required for the 1D cooling channel analysis includes the configuration and material of the cooling channel and thrust chamber, combustion gas properties, and coolant properties. The configuration and material of the cooling channel and thrust chamber are presented in references [5,6]. The combustion gas properties were calculated using RPA [14], and coolant properties were calculated using CoolProp [15].

Inside the cooling channel, the coolant moves from the nozzle exit to the combustion chamber; therefore, the analysis proceeds from the nozzle exit to the combustion chamber, as shown in Fig. 3. Eq. 13 presents the heat transfer analysis for the cooling jacket. The analysis assumes gas-side wall temperature at the starting position (T_{wg}) and calculates T_{aw} and the heat transfer coefficient (h_g) of the hot side by using the hot gas properties at the center of the nozzle. Subsequently, the heat resistance (R_w, R_t) and the heat transfer coefficient (h_c) of the

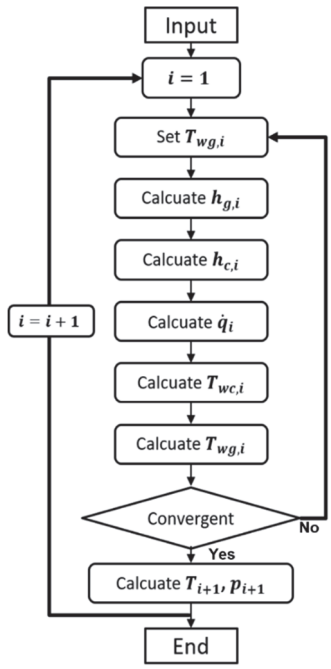

Fig. 4. Calculation procedure of heat transfer analysis.

coolant side are calculated using the configuration and material of the cooling channel and the properties of the coolant. The Dittus-Boelter equation is used to calculate the heat transfer coefficient between the coolant side and the inner wall, and the fin efficiency of the cooling channel was considered [16]. Finally, each wall temperature ($T_{wg,cal}$, T_{wg}) was calculate using Eq. 17-19.

$$\dot{q} = \frac{1}{R_t}(T_{aw} - T_{co}) = h_g(T_{aw} - T_{wg}) = h_c(T_{wc} - T_{co}) \quad (13)$$

$$T_{aw} = T_t\left(\frac{1+Pr^{1/3}\frac{\gamma-1}{2}M^2}{1+\frac{\gamma-1}{2}M^2}\right) \quad (14)$$

$$R_w = \frac{t}{k_w} \quad (15)$$

$$R_t = \frac{1}{h_g} + R_w + \frac{1}{h_c} \quad (16)$$

$$\dot{q} = \frac{T_{aw} - T_{co}}{R_t} \quad (17)$$

$$T_{wg,cal} = T_{aw} - \frac{\dot{q}}{h_g} \quad (18)$$

$$T_{wc} = T_{co} + \frac{\dot{q}}{h_c} \quad (19)$$

$$T_{co,i+1} = T_{co,i} + \frac{\dot{q}_i A_{local,i}}{\dot{m} C_{p\,co,i}} \quad (20)$$

This is repeated until the gas-side wall temperature converges; if the difference between the set gas-side wall temperature and the calculated gas-side wall temperature is below a value of 10^{-4}, it is considered to converge, and the analysis of the following position is conducted.

For the calculation of the following location, the temperature increase ($\dot{q}_i A_{local,i}/\dot{m} C_{p\,co,i}$) of the coolant is calculated using the heat flux, the area of the inner wall of the cooling channel at the location, the specific heat of the coolant, and the mass flow rate in the cooling channel. This temperature increase is reflected in the coolant temperature at the corresponding location to calculate the coolant temperature at the following location in Eq. 20. Simultaneously, the pressure at the next position is calculated by the pressure drop inside the cooling channel using the Darcy-Weisbach equation. The gas-side wall temperature for the first iteration uses the converged value of the previous position (T_{wg}).

3.3 Simulation results

3.3.1 Validation

For the validation of the analysis procedure performed in this study, heat transfer analysis for a regenerative cooling nozzle using liquid methane fuel was performed, and the results obtained by Betti [5] and the simulation results by the author using the commercial program (RPA [14]) were compared.

Betti obtained combustion gas properties using NASA CEA and performed hot gas flow RANS analysis for the combustion chamber and nozzle [5]. Quasi-2D simulation with 1D mass conservation, momentum balance, and 2D energy balance, including the radial direction, was used for cooling channel analysis. In the analysis, CFD and Eq. 6 were used for each heat transfer coefficient. RPA [14], which is used to compare the results, can be divided primarily into the performance analysis of rocket engines and 1D thermal analysis. The combustion pressure, propellant conditions, chamber configuration, and nozzle conditions were used as inputs for performance analysis. The 1D thermal analysis derives the heat transfer coefficient using the combustion gas properties of the performance analysis. It uses the nozzle configuration and region of the cooling channel, material properties of the coolant, flow rate, and flow direction as inputs. The configuration of the combustion chamber and nozzle, thrust and specific impulse, and combustion gas properties at each location are derived as outputs. Furthermore, at each location, the heat transfer coefficient, heat flux, gas-side wall temperature, and coolant properties were derived as the output. The heat transfer coefficient used is calculated through Eq. 6. The heat transfer analysis of the cooling channel proceeds in the same direction as the flow of the coolant, and at each location, the heat transfer coefficient and the properties of the coolant were used to repeat the calculation until the gas-side wall temperature converged. After the convergence, the properties were used to derive the coolant properties at the following location. Table 3 shows the differences between the results obtained using the 1D analysis procedure presented in 3.2 and the results using RPA compared to the Betti's results [5]. The same heat transfer coefficient of Eq 6 was applied for a

Table 3. Differences of properties by simulations.

Results \ Location		Coolant Outlet	Nozzle Throat	Coolant Inlet
$\dot{q}$	Present	7.9%	6.0%	25.6%
	RPA	5.3%	2.9%	35.3%
T_{wg}	Present	8.0%	-14.1%	20.9%
	RPA	8.6%	-9.5%	35.3%
T_{co}	Present	8.0%	2.5%	-
	RPA	3.1%	1.8%	-
P_{co}	Present	1.8%	-0.01%	-
	RPA	-2.3%	0.05%	-

comparison. At the coolant inlet, the temperature and pressure of the coolant were the input conditions. The differences in the heat flux and gas-side wall temperature were relatively large at the coolant inlet location, however only the gas-side temperature was approximately 14% without any significant difference in other locations. The difference of the heat flux and the gas-side wall temperature respectively has almost no absolute difference in value between the inlet and outlet positions, however the reference value for comparison is too small to show a large error. The results show that the presented procedure for the heat transfer analysis is valid through a comparison with the results using RPA [14] and Betti's quasi-2D analysis. Furthermore, the differences in the semi-empirical heat transfer coefficients were analyzed based on this result.

3.3.2 Effect of semi-empirical equations on heat transfer in a regenerative cooling

The heat transfer analysis was performed with various semi-empirical heat transfer coefficients for the cooling channel of a liquid rocket nozzle. The characteristics of the semi-empirical equations was analyzed by comparison with the CFD results. Various semi-empirical equations mentioned in Section 2 were compared. Except for the coolant pressure, all of the results, such as heat transfer coefficient, heat flux, gas-side wall temperature, and coolant temperature, are lower in the CFD-based results than in the semi-empirical equations-based results; however, there is a semi-empirical equation with similar results to the CFD-based analysis results.

Fig. 5 shows the heat transfer coefficient with the semi-empirical equations and CFD results. Among the semi-empirical equations, the Bartz equation in Eqs. 6 and 5 is slightly different depending on the existence of the $(D_*/r_c)^{0.1}$ term. As aforementioned, the modified Bartz equation, Eq. 8 is derived from the Bartz equation of Eq. 6 using the calculation of σ. Eq. 11 is another modified Bartz equation with a temperature correction factor(K_T).

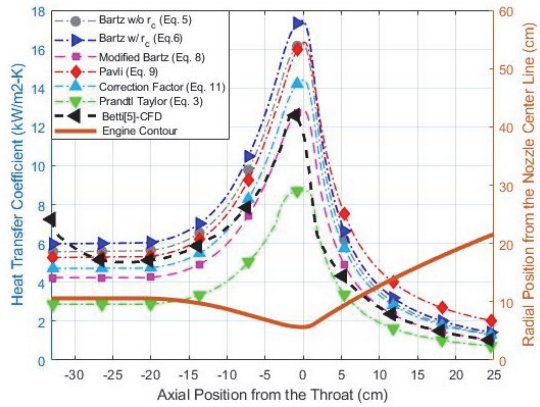

Fig. 5. Heat transfer coefficient with analysis method.

The Pavli equation in Eq. 9 is the Nusselt number-based semi-empirical equation, however it has $c = 0.023$ with the difference in the exponent of the A_*/A term compared with Eq. 5. Therefore, near the nozzle throat region, the results have different values compared with the other equations depending on the location. Therefore, the calculated value of the heat transfer coefficient decreases in the order of Bartz equation with r_c (Eq. 6), Pavli equation in Eq. 9, Bartz equation without r_c (Eq. 5), modified Bartz equation with a temperature correction factor in Eq. 11, modified Bartz equation in Eq. 8, and Prandtl-Taylor analogy. Compared with Betti's CFD results [5], the results show that the modified Bartz equation in Eq. 8 were the most similar. This is because of substituting a value in Eq. 6 in the process of deriving to Eq. 8, whereas ω of the σ term in Eq. 7 is assumed in Eq. 6.

In Fig. 6, the heat flux and gas-side wall temperature exhibit a similar tendency with the semi-empirical heat transfer coefficient. In the analysis, heat transfer coefficient requires gas-side wall temperature, heat flux requires heat transfer coefficient, and gas-side wall temperature requires heat flux and heat transfer coefficient, respectively, in the process. For this reason, each process interacted during the analysis. For the heat flux analysis results, the modified Bartz equation in Eq. 8 was close to the CFD result obtained

by Betti [5], and for the gas-side wall temperature, the coolant temperature increases at the nozzle outlet. As the

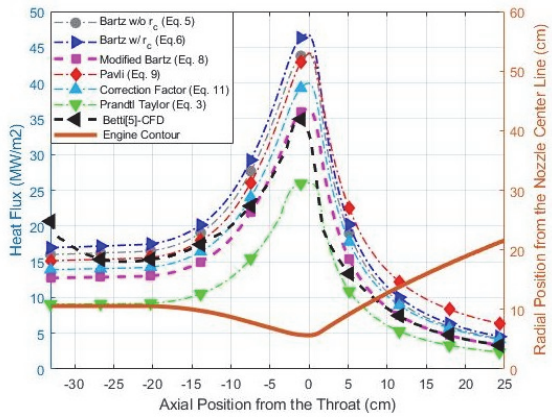

(a) Heat flux

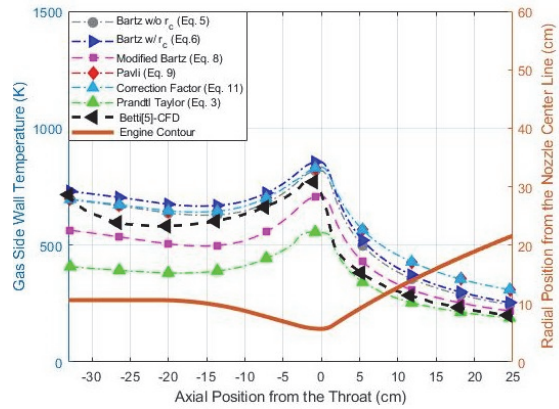

(b) Gas-side wall temperature

Fig. 6. Heat flux and gas-side wall temperature with analysis method.

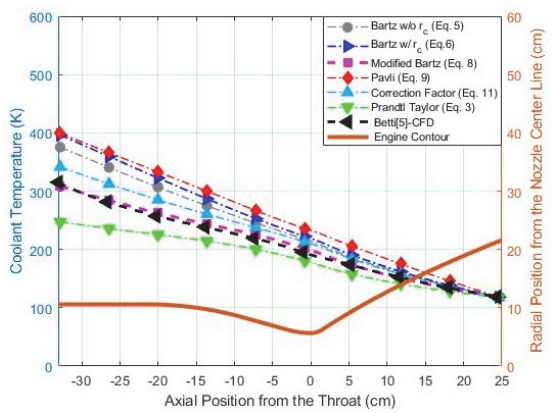

Fig. 7. Coolant temperature with analysis method.

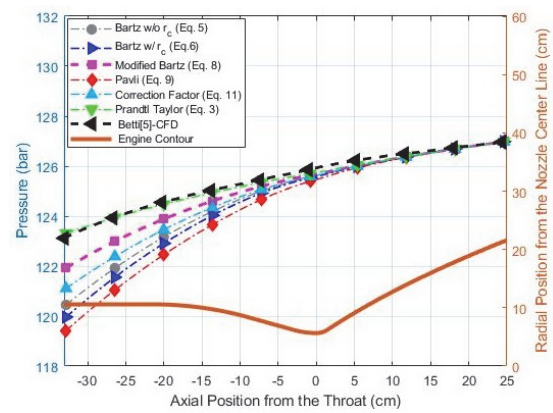

Fig. 8. Coolant pressure with analysis method.

modified Bartz equation with a temperature correction factor in Eq. 11 was close to that of Betti [5]. Therefore, selecting a semi-empirical equation for the target result, such as heat flux result, can decrease the difference between 1D analysis and CFD result.

The temperature and pressure of the coolant inside the channel are shown in Figs. 7 and 8, respectively. At the beginning of the cooling channel, the Pavli equation of Eq. 9 shows a higher heat transfer coefficient than other semi-empirical equations because of the temperature correction factor. This induces a considerable pressure drop as the analysis proceeds, the effect increases from the nozzle exit to the chamber direction. As a result, a high outlet temperature and a significant pressure drop appeared in comparison to other semi-empirical equations. Therefore, the temperature increase and pressure drop in the cooling channel show a similar trend with the heat transfer coefficient, and it can also be shown as the temperature increases and pressure drop in the Pavli equation(Eq. 9) is higher than that of the Bartz equation with r_c(Eq. 6). Although these two semi-empirical equations are slightly different, both have a higher pressure drop than Betti's

Table 4. Average differences between semi-empirical equations and reference.

Property / Equation	h_g	q	T_{wg}	T_{co}	P_{co}
Eq. 5	23.3	20.6	15.6	11.7	-0.06
Eq. 6	32.4	23.2	21.4	15.3	-0.71
Eq. 8	-4.6	-3.8	-3.0	1.2	-0.32
Eq. 9	39.2	34.2	26.7	20.7	-0.90
Eq. 11	10.3	9.5	7.3	7.4	-0.50
Eq. 3	-34.4	-31.7	-22.9	-9.3	-0.07

result[5]. On the contrary, the results of the modified Bartz equation of Eq. 8 are almost identical to Betti's CFD results[5]. One of the reasons for this is that the analysis result of Betti[5] has a lower pressure drop and coolant temperature results using semi-empirical equations. Consequently, the modified Bartz equation of Eq. 8 show that the results of heat transfer coefficient, heat flux, and coolant temperature are closest to the Betti's CFD simulation and appear to have an advantage in predicting the heat transfer coefficient and the properties of the outlet of the cooling channel. Additionally, it can be compared quantitatively through Table 4, which shows the average differences in percent between semi-empirical equations and Betti's CFD results.

4. Conclusions

For the heat transfer analysis of regenerative cooling jacket, different semi-empirical heat transfer coefficients in the liquid rocket nozzle were applied to the liquid methane rocket engine. The axial direction of the regenerative cooling nozzle was subjected to a 1D heat transfer analysis, and various semi-empirical heat transfer coefficients were compared. The results of the 1D analysis are comparable to CFD results. The results revealed that the heat transfer coefficients differ from the empirical method, and these differences affect the heat flux, gas-side wall temperature, and coolant temperature and pressure. The Prandtl-Taylor analogy showed a lower heat transfer coefficient and wall temperature at the nozzle throat than the results from quasi-2D CFD results. The heat transfer coefficient predicted using the modified Bartz equation of Eq. 8 showed a value close to the CFD result after the convergent part of the nozzle, and the coolant pressure and temperature were consistent at all locations.

Acknowledgements

This research was supported by the Space Challenge Project through the National Research Foundation of Korea (NRF-2021M1A3B8078916) with funding from the Korean government (Ministry of Science and ICT) in 2021.

References

1. Shine, S.R. and Nidhi, S.S, "Review on film cooling of liquid rocket engines," Propulsion and Power Research, Vol. 7, Issue 1, pp. 1-18, 2018.
2. Pizzarelli, M., Nasuti, F. and Onofri, M., "CFD Analysis of Curved Cooling Channel Flow and Heat Transfer in Rocket Engines," 46*th AIAA/SAE/SAEE Joint Propulsion Conference & Exhibit*, Nashville, T.N., U.S.A., AIAA 2010-6722, Jul. 2010.
3. Ulas, A. and Boysan, E., "Numerical analysis of regenerative cooling in liquid propellant rocket engines," *Aerospace Science and Technology*, Vol. 24, Issue 1, pp. 187-197, Feb. 2013.
4. Cavillon, R., Haraghi, M.H. and Chen, G., "Comparison of Heat Transfer Characteristic of Rectangular and Oval Cooling Channels of Regeneratively Cooled Rocket Engines," *51th AIAA/SAE/SAEE Joint Propulsion Conference*, Orlando, F.L., U.S.A., AIAA 2015-3759, Jul. 2015.

5. Betti, B., "Flow Field and Heat Transfer Analysis of Oxygen/Methane Liquid Rocket Engine Thrust Chambers," Ph.D. Dissertation, Department of Mechanical and Aerospace Engineering, Universita di Roma "La Sapienza", Roma, Italia, 2012.
6. Schuff, R., Maier, M., Sindiy, O., Ulrich, C. and Fugger, S., "Integrated Modeling and Analysis for a LOX/Methane Expander Cycle Engine: Focusing on Regenerative Cooling Jacket Design," *42nd AIAA/ASME/SAE/ASEE Joint Propulsion Conference and Exhibit*, Sacramento, C.A., U.S.A., AIAA 2006-4534, Jul. 2006.
7. Bartz, D. R., "A simple equation for rapid estimation of rocket nozzle convective heat transfer coefficients," *Jet Propulsion*, Vol. 27, No. 1, pp. 49-51, Jan. 1957.
8. Bartz, D. R., "Turbulent Boundary-Layer Heat Transfer from Rapidly Acceleration Flow of Rocket Combustion Gases and of Heated Air," *Advances in Heat Transfer*, Vol. 2, pp. 2-108, 1965.
9. Huzel, D.K. and Huang, D.H., *Modern engineering for design of liquid-propellant rocket engines*, American Institute of Aeronautics and Astronautics, U.S.A., 1992.
10. Pavli, A.J., Curley, J.K, Masters, P.A and Schwartz, R.M., "Design and Cooling Performance of A Dump-Cooled Rocket Engine," NASA TN-D-3532, 1966.
11. Astrium and TU Dresden., "Final report on data correlation and evaluation of test results phase 1 part 1,". Astrium GSTP-2-TN-06, 2001.
12. Di Matteo, F., De Rosa, M. and Onofri, M., "Semi-empirical heat transfer correlations in combustion chambers for transient system modelling," Space Propulsion Conference 2010, San Sebastian, Spain, May 2010.
13. Adami, A., Mortazavi, M. and Nosratollahi, M., "Heat Transfer Modeling of Bipropellant Thrusters for using in Multidisciplinary Design Optimization Algorithm," *Journal of Fluid Flow, Heat and Mass Transfer*, Vol. 2, pp. 40-46, 2015.
14. Ponomarenko A. "RPA: Tool for Rocket Propulsion Analysis. Thermal Analysis of Thrust Chambers," RP Software+Engineering UG, Neunkirchen-Seelscheid, Germany, 2012.
15. Bell, I.H., Wronski, J., Quoilin, S. and Lemort, V., "Pure and Pseudo-pure Fluid Thermophysical Property Evaluation and the Open-Source Thermophysical Property Library CoolProp," *Industrial & Engineering Chemistry Research*, Vol. 53, Issue 6, pp. 2498-2508, Jan. 2014.
16. Incropera, F.P., Dewitt, D.P., Bergman, T.L and Lavine, A.S, *Fundamentals of Heat and Mass Transfer*, 6th ed., John Wiley & Sons Inc., New York, N.Y., U.S.A., 2006.